AIMS Mathematics, 9(9): 24699–24721.
DOI: 10.3934/math.20241203
Received: 23 May 2024
Revised: 12 July 2024
Accepted: 08 August 2024
Published: 22 August 2024

https://www.aimspress.com/journal/Math

Research article

The fractional soliton solutions: shaping future finances with innovative wave profiles in option pricing system

Hamood Ur Rehman[1], **Patricia J. Y. Wong**[2,*], **A. F. Aljohani**[3], **Ifrah Iqbal**[1] **and Muhammad Shoaib Saleem**[1]

[1] Department of Mathematics, University of Okara, Okara, Pakistan

[2] School of Electrical and Electronic Engineering, Nanyang Technological University, Singapore

[3] Department of Mathematics, Faculty of Science, University of Tabuk, Tabuk, Saudi Arabia

* **Correspondence:** Email: ejywong@ntu.edu.sg.

Abstract: Financial engineering problems hold considerable significance in the academic realm, where there remains a continued demand for efficient methods to scrutinize and analyze these models. Within this investigation, we delved into a fractional nonlinear coupled system for option pricing and volatility. The model we examined can be conceptualized as a fractional nonlinear coupled wave alternative to the governing system of Black-Scholes option pricing. This introduced a leveraging effect, wherein stock volatility aligns with stock returns. To generate novel solitonic wave structures in the system, the present article introduced a generalized Ricatti mapping method and new Kudryashov method. Graphical representations, both in 3D and 2D formats, were employed to elucidate the system's response to pulse propagation. These visualizations enabled the anticipation of appropriate parameter values that align with the observed data. Furthermore, a comparative analysis of solutions was presented for different fractional order values. Additionally, the article showcases the comparison of wave profiles through 2D graphs. The results of this investigation suggested that the proposed method served as a highly reliable and flexible alternative for problem-solving, preserving the physical attributes inherent in realistic processes. To sum up, the main objective of our work was to conceptualize a fractional nonlinear coupled wave system as an alternative to the Black-Scholes option pricing model and investigate its implications on stock volatility and returns. Additionally, we aimed to apply and analyze methods for generating solitonic wave structures and compare their solutions for different fractional order values.

Keywords: Black-Scholes equation; option pricing modelling; generalized Ricatti mapping method (GREM); new Kudryashov's method (NKM); M-truncated fractional derivative
Mathematics Subject Classification: 35C05, 35C08

1. Introduction

In recent decades, corporations have sought crucial instruments to manage financial securities. Within the realm of financial securities, options play a pivotal role in mitigating risks arising from fluctuations in stock prices [1]. To delve into the diverse alternatives available for these options, Lesmana and Wang [2] categorize them into two primary types: European options, which can be executed solely on a specific date, known as the expiry date, and American options, which offer the flexibility of exercise either on or before the expiry date. A crucial economic concern for both traders and investors revolves around establishing a reliable methodology for pricing options, determining the suitable theoretical value for call or put options. Over time, the conceptualization of options as a comprehensive financial instrument was not common place among traders, and the valuation of options remained a formidable and intricate challenge. In [3], pricing options involves the application of mathematical models that frequently pose significant challenges in terms of solution.

Over the past five decades, various endeavors have been made to introduce alternative methods for option pricing. Notably, a groundbreaking advancement occurred in 1973 when Black and Scholes [4] proposed a mathematical model to compute a fair value for options. According to their seminal work [4], the Black-Scholes model represents a pure log-normal diffusion model, resulting in a parabolic partial differential equation within the framework of Ito's calculus. Another noteworthy contribution came from Merton [5], who expanded upon the model equation initially proposed by Black and Scholes. Black and Scholes demonstrated that their formulae related to partial differential equations which effectively determine a fair value for both call and put options. The well-known Black-Scholes option pricing model, commonly referred to as Black-Scholes-Merton, is defined by the equation [6]

$$A(t) + \sigma^2 \frac{2s^2 A_{xx}}{r} + rA_x - rA = 0. \tag{1.1}$$

The stock price S follows a geometric Brownian motion, described by the stochastic differential equation:

$$dS = \mu S\, dt + \sigma S\, dW(t), \tag{1.2}$$

where μ represents the instantaneous mean return, σ is the stock volatility, and $W(t)$ is a Wiener process. The Black-Scholes model has sparked significant interest, leading to advancements in financial mathematics and engineering. However, it has limitations in pricing unconventional option types such as American or Asian options due to its inability to account for exercise features and path dependencies. Moreover, an obstacle highlighted by Lesmana and Wang [2] is the diminished validity of the Black-Scholes option pricing methodology in the presence of transaction costs associated with trading in risk-free securities or stocks. To address this point, different models have been introduced by researchers such as Boyle and Vorst [7], Leland [8], Barles and Soner [9] and Kusuoka [10]. Ivancevic has recently introduced an option pricing model [11]. This model is grounded in the Elliott wave market theory [12], Lo's contemporary adaptive market hypothesis [13], and the quantum neural computation approach [14]. Ivancevic's model is read as [15–17]

$$\iota B(t) + \sigma^2 B_{xx} + \beta |B|^2 B = 0, \tag{1.3}$$

which aims to capture the behavioral complexities and efficient market dynamics. Here, σ denotes volatility (which can be constant or a stochastic process), $B(x,t)$ represents the option price wave function, and β signifies the adaptive market potential coefficient.

The Black-Scholes model, defined by Eqs (1.1) and (1.2), assumes constant volatility and is primarily suited for European options, however it fails to capture market behaviors such as stochastic volatility and path dependencies. Ivancevic's model introduces nonlinear dynamics with Eq (1.3) and further proposes a coupled nonlinear model for both volatility and option pricing, as detailed in [18, 19], thereby capturing the independencies between these factors. By introducing an adaptive market potential coefficient β that varies with market conditions, this model offers a more accurate and realistic approach to option pricing, expressed as follows:

$$\iota U_t + \frac{1}{2}U_{xx} + \beta(|U|^2 + |V|^2)U = 0, \tag{1.4}$$

$$\iota V_t + \frac{1}{2}V_{xx} + \beta(|U|^2 + |V|^2)V = 0. \tag{1.5}$$

In its fractional form, the model is written as [19]

$$\iota D_t^{M,\alpha} U + \frac{1}{2}U_{xx} + \beta(|U|^2 + |V|^2)U = 0, \tag{1.6}$$

$$\iota D_t^{M,\alpha} V + \frac{1}{2}V_{xx} + \beta(|U|^2 + |V|^2)V = 0. \tag{1.7}$$

Here, Eqs (1.6) and (1.7) represent the volatility model and the option pricing model, respectively. $U(x,t)$ represents the option pricing wave function, while $V(x,t)$ represents the volatility wave function. $D_t^{M,\alpha}$ denotes the M-truncated fractional derivative [20] having order α.

Fractional calculus, originally designed for the formulation of non-integer derivatives and integrals, presents a robust mathematical framework for explicating a myriad of phenomena across different scientific domains [21, 22]. This increasing prominence is fueled by the escalating demand for precise simulations of both historical and contemporary physical phenomena [23–25]. Studies have demonstrated the utility of fractional operators in modeling natural phenomena, highlighting that fractional-order models surpass non-integer (classical) systems in effectiveness and productivity [26, 27].

Different techniques are used to solve the nonlinear fractional partial differential equations such as the extended hyperbolic function method [28–30], Sardar sub-equation method [31, 32], Kudryashov's method [33, 34], Bernoulli sub-ODE method [35, 36], Jacobi's elliptic function [37, 38], new extended direct algebraic method [39, 40], mapping method [41–44], and the ϕ^6-expansion method [45]. In the present paper, the option pricing model in the sense of M-truncated fractional derivative [20] is solved by using the generalized Ricatti equation mapping method (GREM) [46, 47] and new Kudryashov method (NKM) [48]. To our knowledge, there is currently no literature addressing analytical solutions for the model under consideration by using these approaches. To fill this void, we utilize these methods to derive comprehensive analytical solutions. The main research questions of our study are: How can a fractional nonlinear coupled wave system serve as an alternative to the Black-Scholes option pricing

model? How effective are the generalized Ricatti mapping method and the new Kudryashov method in generating novel solitonic wave structures in the fractional nonlinear coupled system? What are the differences in the system's response to pulse propagation when visualized through 3D and 2D graphical representations? How do solutions vary for different fractional order values, and what insights can be drawn from comparing wave profiles through 2D graphs?

The contribution made by this paper holds significant relevance in several respects. First of all, it broadens the analytical toolbox for solving nonlinear fractional partial differential equations, which are used in a variety of scientific fields and go beyond financial modeling. Second, by concentrating on option pricing, a crucial component of financial markets–the study tackles a relevant issue that traders and investors encounter in the real world. Third, the model gains sophistication from the use of M-truncated fractional derivatives, which better captures the dynamics of volatility and option pricing. Lastly, the derivation of thorough analytical solutions closes a significant gap in the literature and provides information that may help financial market decision-making processes.

The remaining paper is structured as follows: Section 2 defines the M-truncated fractional derivative with properties. Section 3 provides mathematical calculation of the governed system. In Section 4, the description and application of GREM are given, while Section 5 describes the NKM with applications. Section 6 is of results and discussion. The conclusion of the paper is provided in Section 7.

2. Preliminary: M-truncated fractional derivative

A completely new variant of the M-fractional derivative is M-truncated fractional derivative [20]. M-truncated fractional differentiation provides a more flexible option by getting rid of the drawbacks of conventional derivatives.

Definition 2.1. Given function $u : [0, \infty) \to \Re$ and an order α, such an M-truncated fractional derivative is defined as follows:

$$D_t^{M,\alpha}u(t) = \lim_{\epsilon \to 0} \frac{u(tE_M(\epsilon t^{-\alpha})) - u(t)}{\epsilon}, \quad t > 0, \quad \alpha > 0.$$

Here, $E_M(t)$ indicates a truncated Mittag-Liffler function, and taking value in the interval (0,1) [49]:

$$E_M(t) = \sum_{n=0}^{\infty} \frac{t^n}{\Gamma(Mn + 1)}.$$

Properties: Suppose that $0 < \alpha \leq 1$, and $l, m \in \Re$. Let u, v be functions such that α-differentiable when $t > 0$:

- $D_t^{M,\alpha}(lu + mv) = lD_t^{M,\alpha}(u) + mD_t^{M,\alpha}(v)$,
- $D_t^{M,\alpha}(uv) = uD_t^{M,\alpha}(v) + vD_t^{M,\alpha}(u)$,
- $D_t^{M,\alpha}(\frac{u}{v}) = \frac{vD_t^{M,\alpha}(u) - uD_t^{M,\alpha}(v)}{v^2}$,
- $D_t^{M,\alpha}(c)$=0.

3. Mathematical analysis

Suppose the following transformation [19]:

$$U(x,t) = Q(\psi)e^{\iota(x+t+\theta)}, \quad V(x,t) = P(\psi)e^{\iota(x+t+\theta)}, \quad \psi = x - \frac{\Gamma(\gamma+1)}{\alpha}(ct^{\alpha}). \tag{3.1}$$

The wave function for option pricing is represented by $U(x,t)$. We define the volatility wave function as $V(x,t)$. The phase component, denoted by θ, determines the wave functions' phase shift. The velocity, or the speed at which the wave travels, is shown by the symbol c. The wave functions' behavior is influenced by the positive parameter γ. The order of the fractional derivative, denoted by α, indicates how persistent or memory-like the price dynamics are. By using (3.1), the following expressions are obtained [19]:

$$\begin{aligned} &D_t^{M,\alpha}U = (cQ' + \iota Q)e^{\iota(x+t+\theta)}, \;\; U_x = (Q' + \iota Q)e^{\iota(x+t+\theta)}, \\ &U_{xx} = (Q'' + 2\iota Q' - Q)e^{\iota(x+t+\theta)}, \;\; |U| = U\overline{U} = U^2, \;\; |V| = V\overline{V} = P^2. \end{aligned} \tag{3.2}$$

By using (3.2) in (1.6) and (1.7), we get

$$\begin{aligned} &-\iota cQ' + \frac{1}{2}Q'' + \iota Q' - \frac{3}{2}Q + \beta(Q^2 + P^2)Q = 0, \\ &-\iota cP' + \frac{1}{2}P'' + \iota P' - \frac{3}{2}P + \beta(Q^2 + P^2)P = 0. \end{aligned} \tag{3.3}$$

The derivation of (3.3) utilizes the definition of the M-truncated fractional derivative as outlined in Section 2 of our paper. The imaginary parts of (3.3) are

$$\begin{aligned} &-\iota cQ' + \iota Q' = 0 \;\; \Rightarrow c = 1, \\ &-\iota cP' + \iota P' = 0 \;\; \Rightarrow c = 1. \end{aligned} \tag{3.4}$$

The real parts of (3.3) are

$$\begin{aligned} &\frac{1}{2}Q'' - \frac{3}{2}Q + \beta(Q^2 + P^2)Q = 0, \\ &\frac{1}{2}P'' - \frac{3}{2}P + \beta(Q^2 + P^2)P = 0. \end{aligned} \tag{3.5}$$

Now, suppose the following transformation [19]:

$$Q = P + \kappa, \tag{3.6}$$

where κ is a real constant. By putting this transformation in the second part of (3.5), we acquire

$$\frac{1}{2}P'' - \frac{3}{2}P + \beta(2P^2 + \kappa^2 + 2\kappa P)P = 0. \tag{3.7}$$

By simplifying, we get

$$P'' + 4\beta P^3 + 4\beta\kappa P^2 + (2\beta\kappa^2 - 3)P = 0. \tag{3.8}$$

4. Description of generalized Riccati equation mapping method

Suppose the solution of (3.8) is

$$P(\psi) = \omega_0 + \sum_{i=1}^{M} \omega_i (Z(\psi))^i, \tag{4.1}$$

where ω_0, ω_i are arbitrary constants and $Z(\psi)$ satisfies the following ODE [46]:

$$Z' = k_1 + k_2 Z + k_3 Z^2, \tag{4.2}$$

where ω_0, ω_i $(i = 1, 2, ..., M)$, k_1, k_2, k_3 are constants that need to be evaluated. The positive integer M can be determined by using the balancing number. By putting (4.1) and (4.2) into (3.8), we will be able to get a set of algebraic equations from which the ω_0, ω_i $(i = 1, 2, ..., M)$, k_1, k_2, k_3 can be determined. The solution of (4.2) has the following cases.

Family 1: When $k_2^2 - 4k_1k_3 > 0$,

$$Z_1 = \frac{-1}{2k_3}\left(k_2 + \sqrt{k_2^2 - 4k_3k_1}\tanh\left(\frac{\sqrt{k_2^2 - 4k_3k_1}}{2}\psi\right)\right), \tag{4.3}$$

$$Z_2 = \frac{-1}{2k_3}\left(k_2 + \sqrt{k_2^2 - 4k_3k_1}\coth\left(\frac{\sqrt{k_2^2 - 4k_3k_1}}{2}\psi\right)\right), \tag{4.4}$$

$$Z_3 = \frac{-1}{2k_3}\left(k_2 + \sqrt{k_2^2 - 4k_3k_1}\left(\tanh\left(\sqrt{k_2^2 - 4k_3k_1}\psi\right) \pm \operatorname{sech}\left(\sqrt{k_2^2 - 4k_3k_1}\psi\right)\right)\right), \tag{4.5}$$

$$Z_4 = \frac{-1}{2k_3}\left(k_2 + \sqrt{k_2^2 - 4k_3k_1}\left(\coth\left(\sqrt{k_2^2 - 4k_3k_1}\psi\right) \pm \operatorname{csch}\left(\sqrt{k_2^2 - 4k_3k_1}\psi\right)\right)\right), \tag{4.6}$$

$$Z_5 = \frac{-1}{4k_3}\left(2k_2 + \sqrt{k_2^2 - 4k_3k_1}\left(\tanh\left(\frac{\sqrt{k_2^2 - 4k_3k_1}}{4}\psi\right) \pm \coth\left(\frac{\sqrt{k_2^2 - 4k_3k_1}}{4}\psi\right)\right)\right), \tag{4.7}$$

$$Z_6 = \frac{1}{2k_3}\left(-k_2 + \frac{\sqrt{(A^2 + B^2)(k_2^2 - 4k_3k_1)} - A\sqrt{k_2^2 - 4k_3k_1}\cosh\left(\sqrt{k_2^2 - 4k_3k_1}\psi\right)}{A\sinh\left(\sqrt{k_2^2 - 4k_3k_1}\psi\right) + B}\right), \tag{4.8}$$

$$Z_7 = \frac{1}{2k_3}\left(-k_2 - \frac{\sqrt{(A^2 + B^2)(k_2^2 - 4k_3k_1)} + A\sqrt{k_2^2 - 4k_3k_1}\cosh\left(\sqrt{k_2^2 - 4k_3k_1}\psi\right)}{A\sinh\left(\sqrt{k_2^2 - 4k_3k_1}\psi\right) + B}\right), \tag{4.9}$$

where $A,\ B \neq 0$ are arbitrary constants and satisfy the condition $A^2 > B^2$,

$$Z_8 = \frac{2k_3\cosh\left(\frac{\sqrt{k_2^2-4k_3k_1}}{2}\psi\right)}{-k_2\cosh\left(\frac{\sqrt{k_2^2-4k_3k_1}}{2}\psi\right) + \sqrt{k_2^2 - 4k_3k_1}\sinh\left(\frac{\sqrt{k_2^2-4k_3k_1}}{2}\psi\right)}, \tag{4.10}$$

$$Z_9 = \frac{-2k_3 \sinh\left(\frac{\sqrt{k_2^2-4k_3k_1}}{2}\psi\right)}{k_2 \sinh\left(\frac{\sqrt{k_2^2-4k_3k_1}}{2}\psi\right) - \sqrt{k_2^2-4k_3k_1}\cosh\left(\frac{\sqrt{k_2^2-4k_3k_1}}{2}\psi\right)}, \tag{4.11}$$

$$Z_{10} = \frac{2k_3 \cosh\left(\frac{\sqrt{k_2^2-4k_3k_1}}{2}\psi\right)}{\sqrt{k_2^2-4k_3k_1}\sinh\left(\sqrt{k_2^2-4k_3k_1}\psi\right) - k_2\cosh\left(\sqrt{k_2^2-4k_3k_1}\psi\right) \pm \iota\sqrt{k_2^2-4k_3k_1}}, \tag{4.12}$$

$$Z_{11} = \frac{2k_3 \sinh\left(\frac{\sqrt{k_2^2-4k_3k_1}}{2}\psi\right)}{-k_2 \sinh\left(\sqrt{k_2^2-4k_3k_1}\psi\right) + \sqrt{k_2^2-4k_3k_1}\cosh\left(\sqrt{k_2^2-4k_3k_1}\psi\right) \pm \iota\sqrt{k_2^2-4k_3k_1}}, \tag{4.13}$$

$$Z_{12} = \frac{4k_3 \sinh(C\psi)\cosh(C\psi)}{-2k_2 \sinh(C\psi)\cosh(C\psi) + 2\sqrt{k_2^2-4k_3k_1}\cosh^2(C\psi) - \sqrt{k_2^2-4k_3k_1}}, \tag{4.14}$$

where $C = \frac{\sqrt{k_2^2-4k_3k_1}}{4}$.

Family 2: When $k_2^2 - 4k_1k_3 < 0$,

$$Z_{13} = \frac{1}{2k_3}\left(-k_2 + \sqrt{4k_3k_1-k_2^2}\tan\left(\frac{\sqrt{4k_3k_1-k_2^2}}{2}\psi\right)\right), \tag{4.15}$$

$$Z_{14} = \frac{-1}{2k_3}\left(k_2 + \sqrt{4k_3k_1-k_2^2}\cot\left(\frac{\sqrt{4k_3k_1-k_2^2}}{2}\psi\right)\right), \tag{4.16}$$

$$Z_{15} = \frac{1}{2k_3}\left(-k_2 + \sqrt{4k_3k_1-k_2^2}\left(\tan\left(\sqrt{4k_3k_1-k_2^2}\psi\right) \pm \sec\left(\sqrt{4k_3k_1-k_2^2}\psi\right)\right)\right), \tag{4.17}$$

$$Z_{16} = \frac{-1}{2k_3}\left(k_2 + \sqrt{4k_3k_1-k_2^2}\left(\cot\left(\sqrt{4k_3k_1-k_2^2}\psi\right) + \csc\left(\sqrt{4k_3k_1-k_2^2}\psi\right)\right)\right), \tag{4.18}$$

$$Z_{17} = \frac{1}{4k_3}\left(-2k_2 + \sqrt{4k_3k_1-k_2^2}\left(\tan\left(\frac{\sqrt{4k_3k_1-k_2^2}}{4}\psi\right) - \cot\left(\frac{\sqrt{4k_3k_1-k_2^2}}{4}\psi\right)\right)\right), \tag{4.19}$$

$$Z_{18} = \frac{1}{2k_3}\left(-k_2 + \frac{\pm\sqrt{(A^2-B^2)(4k_3k_1-k_2^2)} - A\sqrt{4k_3k_1-k_2^2}\cos\left(\sqrt{4k_3k_1-k_2^2}\psi\right)}{A\sin\left(\sqrt{4k_3k_1-k_2^2}\psi\right)+B}\right), \tag{4.20}$$

$$Z_{19} = \frac{1}{2k_3}\left(-k_2 - \frac{\pm\sqrt{(A^2-B^2)(4k_3k_1-k_2^2)} + A\sqrt{4k_3k_1-k_2^2}\cos\left(\sqrt{4k_3k_1-k_2^2}\psi\right)}{A\sin\left(\sqrt{4k_3k_1-k_2^2}\psi\right)+B}\right), \tag{4.21}$$

where $A,\ B \neq 0$ are arbitrary constants and satisfy the condition $A^2 > B^2$,

$$Z_{20} = -\frac{2k_3\cos\left(\frac{\sqrt{4k_3k_1-k_2^2}}{2}\psi\right)}{k_1 cos\left(\frac{\sqrt{4k_3k_1-k_2^2}}{2}\psi\right) + \sqrt{4k_3k_1-k_2^2}\sin\left(\frac{\sqrt{4k_3k_1-k_2^2}}{2}\psi\right)}, \tag{4.22}$$

$$Z_{21} = \frac{2k_3\sin\left(\frac{\sqrt{4k_3k_1-k_2^2}}{2}\psi\right)}{k_1\sin\left(\frac{\sqrt{4k_3k_1-k_2^2}}{2}\psi\right) + \sqrt{4k_3k_1-k_2^2}\cos\left(\frac{\sqrt{4k_3k_1-k_2^2}}{2}\psi\right)}, \tag{4.23}$$

$$Z_{22} = -\frac{2k_3\cos\left(\frac{\sqrt{4k_3k_1-k_2^2}}{2}\psi\right)}{\sqrt{4k_3k_1-k_2^2}\sin\left(\sqrt{4k_3k_1-k_2^2}\psi\right) + k_1\cos\left(\sqrt{4k_3k_1-k_2^2}\psi\right) \pm \iota\sqrt{4k_3k_1-k_2^2}}, \tag{4.24}$$

$$Z_{23} = \frac{2k_3\sin\left(\frac{1}{2}\sqrt{4k_3k_1-k_2^2}\psi\right)}{-k_2\sin\left(\sqrt{4k_3k_1-k_2^2}\psi\right) - \sqrt{4k_3k_1-k_2^2}\cos\left(\sqrt{4k_3k_1-k_2^2}\psi\right) \pm \iota\sqrt{4k_3k_1-k_2^2}}, \tag{4.25}$$

$$Z_{24} = \frac{4k_3\sin\left(\frac{\sqrt{4k_3k_1-k_2^2}}{4}\psi\right)\cos\left(\frac{\sqrt{4k_3k_1-k_2^2}}{4}\psi\right)}{-2k_2\sin\left(\frac{\sqrt{4k_3k_1-k_2^2}}{4}\psi\right)\cos\left(\frac{\sqrt{4k_3k_1-k_2^2}\psi}{4}\right) + 2\sqrt{4k_3k_1-k_2^2}\cos^2\left(\frac{\sqrt{4k_3k_1-k_2^2}\psi}{4}\right) - \sqrt{4k_3k_1-k_2^2}}. \tag{4.26}$$

Family 3: When $k_3 = 0$ and $k_2k_1 \neq 0$,

$$Z_{25} = \frac{-k_2 d}{k_1(d + \cosh(k_2\psi) - \sinh(k_2\psi))}, \tag{4.27}$$

$$Z_{26} = \frac{k_2(\cosh(k_2\psi) + \sinh(k_2\psi))}{k_1(d + \cosh(k_2\psi) + \sinh(k_2\psi))}, \tag{4.28}$$

where d is any arbitrary constant.

Family 4: When $k_2 = 0$, $k_3 = 0$, and $k_1 \neq 0$,

$$Z_{27} = \frac{-1}{c_1 + k_1\psi}, \tag{4.29}$$

where c_1 is an arbitrary constant. By inserting these cases and values of constant in (4.1), we can obtain the solutions of (1.6) and (1.7).

Note: The Families 1–4 represent specific sets of solutions that satisfy (4.2) under certain conditions. These families are not only identified within the context of our study but have also been extensively studied and utilized in the literature [46].

4.1. Application of generalized Riccati equation mapping method

By employing the homogeneous balancing rule on Eq (3.8), focusing on the terms with the highest order and nonlinearity, namely, P'' and P^3, we deduce the equation $M + 2 = 3M$, which gives $M = 1$. Thus, referencing (4.1), we deduce

$$P(\psi) = \omega_0 + \omega_1 Z(\psi). \tag{4.30}$$

Now, by putting (4.30) and (4.2) into (3.8), and equating the coefficients of $(Z(\psi))^i$, i=0,1,2,3 to zero, we establish the following algebraic system:

$$\begin{aligned}
&(Z(\psi))^0 : \left(3\beta\kappa^2 - 2\right)\omega_0 + 4\beta\kappa\omega_0^2 + 4\beta\omega_0^3 + k_1k_2\omega_1 = 0,\\
&(Z(\psi))^1 : \omega_1\left(3\beta\kappa^2 - 2\right) + 8\beta\kappa\omega_0\omega_1 + 12\beta\omega_0^2\omega_1 + 2k_1k_3\omega_1 + r^2\omega_1 = 0,\\
&(Z(\psi))^2 : 4\beta\kappa\omega_1^2 + 12\beta\omega_0\omega_1^2 + 3k_2k_2\omega_1 = 0,\\
&(Z(\psi))^3 : 4\beta\omega_1^3 + 2k_3^2\omega_1 = 0.
\end{aligned}$$

By solving this system, the following values of constants are obtained:

$$k_3 = \frac{\omega_1\left(10\beta\omega_0 + \sqrt{30}\sqrt{\beta}\right)}{\sqrt{5}\sqrt{-10\beta\omega_0^2 - 2\sqrt{30}\sqrt{\beta}\omega_0 - 3}},\quad k_1 = -\frac{2\omega_0\left(5\sqrt{\beta}\omega_0 + \sqrt{30}\right)\sqrt{-10\beta\omega_0^2 - 2\sqrt{30}\sqrt{\beta}\omega_0 - 3}}{5\omega_1\left(2\sqrt{5}\sqrt{\beta}\omega_0 + \sqrt{6}\right)},$$

$$k_2 = -2\sqrt{-2\beta\omega_0^2 - 2\sqrt{\frac{6}{5}}\sqrt{\beta}\omega_0 - \frac{3}{5}},\quad \kappa = \frac{3\sqrt{\frac{3}{10}}}{\sqrt{\beta}}.$$

In the given solution sets, ω_0 and ω_1 are indeed known constants, while the values of the other constants depend on them. Typically, these values are chosen in accordance with the conditions of the method. While they can be selected somewhat randomly, it is important to ensure that their values do not violate the conditions necessary for the method to be applied effectively. Now, by inserting these values of constants in (4.3)–(4.29) and by using (4.30) and (3.6), we can find the following solutions of (1.6) and (1.7). For j=1,2,...,27, the solutions of (1.6) and (1.7) can be obtained as

$$\begin{aligned}
V_j &= (\omega_0 + \omega_1 Z_j)e^{\iota(x+t+\theta)},\\
U_j &= (\omega_0 + \omega_1 Z_j + \kappa)e^{\iota(x+t+\theta)},
\end{aligned}$$

where Z_j's are given in (4.3)–(4.29).

5. New Kudryashov's method

Let the solution of (3.8) be

$$P(\psi) = \sum_{i=1}^{M} a_i (G(\psi))^i, \tag{5.1}$$

where a_i $(i = 1, 2..., M)$ are constants. M can be obtained by using the homogeneous balancing rule and $G(\psi)$ satisfies the following ODE [48]:

$$G'(\psi)^2 = \delta^2 G(\psi)^2 (1 - \chi G(\psi)^2), \tag{5.2}$$

where δ, χ are constants and the solution of (5.2) is

$$G(\psi) = \frac{4L}{4e^{\delta\psi} L^2 + e^{-\delta\psi}\chi}, \tag{5.3}$$

where L is the integration constant [48]. Now, by inserting (5.1) and (5.2) into (3.8), the system of equations is attained, and by solving it, we get the values of constants.

5.1. Application of new Kudryashov's method

By using the homogeneous balancing rule as discussed in Section 4.1, we let the following be the solution of (3.8):

$$P(\psi) = a_0 + a_1 G(\psi). \tag{5.4}$$

Now, by putting (5.4) and (5.3) into (3.8), and equating the coefficients of $(G(\psi))^i$, i=0,1,2,3 to zero, we establish the following algebraic system:

$$\begin{aligned}
&(G(\psi))^0 : 4a_0^3\beta + 4a_0^2\beta\kappa + 2a_0\beta\kappa^2 - 3a_0 = 0,\\
&(G(\psi))^1 : 12a_0^2\beta a_1 + 8a_0\beta a_1\kappa + 2\beta a_1\kappa^2 + a_1\delta^2 - 3a_1 = 0,\\
&(G(\psi))^2 : 12a_0\beta a_1^2 + 4\beta a_1^2\kappa = 0,\\
&(G(\psi))^3 : 4\beta a_1^3 - 2a_1\delta^2\chi = 0.
\end{aligned}$$

We get the following values of constants by solving the above system:

$$\delta = \sqrt{\frac{6}{5}}, \quad a_0 = -\frac{1}{\sqrt{10\beta}}, \quad \kappa = \frac{3\sqrt{\frac{3}{10}}}{\sqrt{\beta}}, \quad a_1 = -\sqrt{\frac{3\chi}{5\beta}}.$$

Now, by inserting these values of constants in (5.4) and by using (3.6), we can find the following solutions of (1.6) and (1.7):

$$V_{1,1}(x,t) = \left(-\frac{1}{\sqrt{10\beta}} - \frac{4L\sqrt{\frac{3\chi}{5}}}{\sqrt{\beta}\left(4L^2 e^{\sqrt{\frac{6}{5}}\psi} + \chi e^{\sqrt{\frac{6}{5}}\psi}\right)}\right) e^{\iota(x+t+\theta)},$$

$$U_{1,1}(x,t) = \left(-\frac{1}{\sqrt{10\beta}} - \frac{4L\sqrt{\frac{3\chi}{5}}}{\sqrt{\beta}\left(4L^2 e^{\sqrt{\frac{6}{5}}\psi} + \chi e^{\sqrt{\frac{6}{5}}\psi}\right)} + \kappa \right) e^{\iota(x+t+\theta)}.$$

In the given set of equations, the parameter χ represents a real-valued constant upon which the value of a_1 depends. In our methodology, we typically consider $\chi = \pm 4L^2$ to ensure a variety of solutions. If we take $\chi = \pm 4L^2$, the obtained solutions are

$$V_{1,2}(x,t) = \left(-\frac{\sqrt{10}\text{sech}\left(\sqrt{\frac{6}{5}}\psi\right) + 1}{\sqrt{10\beta}} \right) e^{\iota(x+t+\theta)},$$

$$U_{1,2}(x,t) = \left(-\frac{\sqrt{10}\text{sech}\left(\sqrt{\frac{6}{5}}\psi\right) + 1}{\sqrt{10\beta}} + \kappa \right) e^{\iota(x+t+\theta)}.$$

$$V_{1,3}(x,t) = \left(-\frac{\sqrt{10}\text{csch}\left(\sqrt{\frac{6}{5}}\psi\right) + 1}{\sqrt{-10\beta}} \right) e^{\iota(x+t+\theta)},$$

$$U_{1,3}(x,t) = \left(-\frac{\sqrt{10}\text{csch}\left(\sqrt{\frac{6}{5}}\psi\right) + 1}{\sqrt{-10\beta}} + \kappa \right) e^{\iota(x+t+\theta)}.$$

6. Results and discussion

Our study introduces the option pricing model within the context of fractional calculus. To be more precise, we add M-truncated fractional derivatives to the conventional option pricing framework, and give a more realistic depiction of the dynamics of financial markets in the option pricing model. To generate analytical solutions for the option pricing model, we apply GREM and NKM. To the best of our knowledge, this is the first time that the particular model under consideration has been used with these solution methods. In [19], the authors first extracted soliton solutions of this model using the ϕ^6 method. In our current study, we applied two different methods, GREM and NKM, which allowed us to extract a wider variety of soliton solutions. While the ϕ^6 method provided an initial framework, our application of GREM and NKM resulted in a more comprehensive set of solutions, including kink, combined dark-bright, combined dark-singular, periodic-singular, and bright solitons. This comparison highlights the enhanced capability of our approach to model complex dynamics within the option pricing framework.

The details of GREM and NKM methods are given in Table 1.

Table 1. Description of methods.

Method	Originality	Advantages and limitations
GREM	Modified version of G'/G expansion method which satisfies $G'' + k_2G + k_3G^2$ [50]. It gives fewer solutions than GREM.	GREM gives 27 different solutions in the form kink, singular, periodic-singular, and combined solution, while it is unable to generate bright soliton solution.
NKM	Modified version of Kudryashov's method which satisfies $\phi'(\psi) = \phi'(\psi)(\phi(\psi) - 1)$ [34].	Generates hyperbolic solutions of different types by changing the values of constants in the form of bright, and singular solitons. This method is unable to extract periodic-singular solutions.

In the ever-evolving landscape of financial markets, the exploration of wave profiles in the option pricing system opens up new frontiers for shaping future finances. The concept of the fractional derivative is used to redefine how we perceive and engage with option pricing and has practical applications across various facets of the financial industry. The integration of fractional calculus into option pricing models enhances risk management strategies, allowing traders and investors to make more informed decisions. By reflecting the complex fractional dynamics present in the market, these models offer more accurate and robust valuation frameworks for options. This optimization ensures that option prices are better aligned with market realities, reduces valuation errors, and improves pricing decisions.

The application of solitons in the Ivancevic option pricing model [11] offers a profound exploration of the nonlinear dynamics having financial derivatives. Solitons play a significant role in unraveling the complexities of option pricing within the context of the proposed model. This investigation into the Ivancevic option pricing model yields diverse range of soliton solutions, including kink, bright, combined dark-bright, combined dark-singular, periodic, and periodic-singular solitons, as shown in Figures 1–6. The visual representation of solitons are given by both 3D and 2D graphical analyses in which the 3D graphs present the perspective on their interaction and behavior in the option pricing system. In a 2D graph, a detailed comparison of two profiles is presented, which focuses on the nuanced changes in amplitude and phase components. Another 2D plot shows the comparison of solutions at different values of fractional order, which illustrates how changes in the order parameter impact soliton properties in the option pricing system.

In Figures 1–6, it is noticed that greater leftward movements are associated with higher α values, suggesting that the form and location of the soliton are more influenced by historical data. On the other hand, smaller α values cause movements to the right, which indicate that historical data has had less of an impact. Furthermore, profile comparison amplitude discrepancies show how the soliton's strength or intensity varies, with larger amplitudes denoting more noticeable disturbances. Through this comparison, traders and investors can gain significant insights into how variations in the fractional order parameter affect the properties of the kink soliton solution within the financial model. The detail of each figure is given below.

The kink soliton solution for V_1 and U_1 is shown in Figure 1. It includes comparisons of V_1 at $\alpha = 0.7$ and $\alpha = 0.4$, as well as 3D plots showing V_1 and U_1 at $\alpha = 0.7$. The term kink soliton in finance refers to a limited wave or disturbance that moves forward without changing its form.

Variations in the position of the soliton graph are noticed in its shifting behavior with changes in the α. The kink soliton solution's use in finance is limited to its ability to forecast specific financial market events. Solitons are waves that move without altering shape and can be related to particular asset price patterns. These might include sudden shifts, which investors must comprehend and account for in their methods. Through the use of the kink soliton solution, analysts may increase the understanding of market phenomena and make better-informed investment choices.

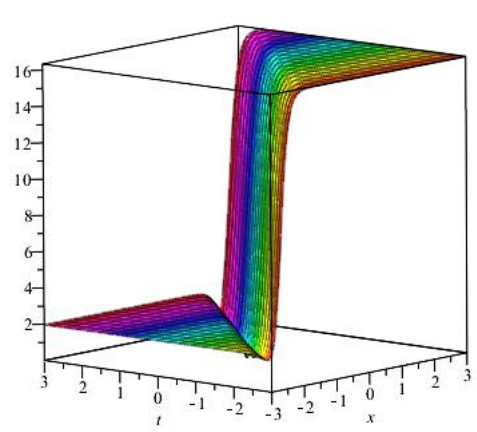

(a) 3D plot V_1 at $\alpha = 0.7$.

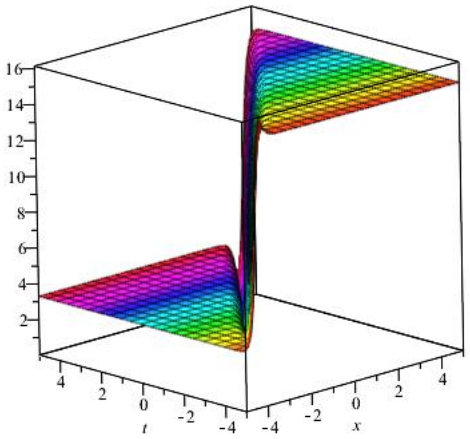

(b) 3D plot U_1 at $\alpha = 0.7$.

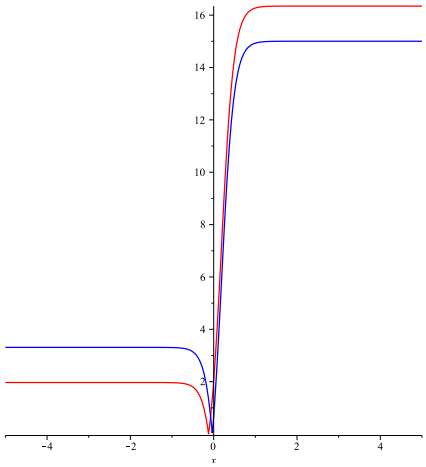

(c) ____ (V_1) ____ (U_1) at $\alpha = 0.7$.

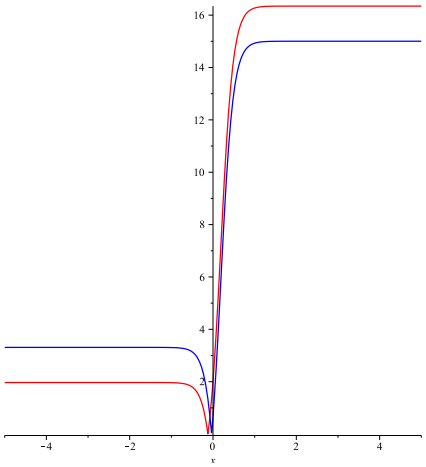

(d) V_1 at ____ $(\alpha = 0.7)$ ____ $(\alpha = 0.4)$.

Figure 1. Graphical representation of kink soliton solution for V_1 and U_1 with $\beta = 1$, $\gamma = 0.6$, $c = 1$, $\theta = 0.8$, $\omega_0 = 0.1$, $\omega_1 = 0.1$, and different values of α.

The combined dark-bright soliton solution for V_3 and U_3 is shown graphically in Figure 2. 3D graphs of V_3 and U_3 at $\alpha = 0.9$, a comparison of their solutions, and a comparison of V_3 at $\alpha = 0.9$ and $\alpha = 0.7$ make up this presentation. Understanding the way that the variables interact in the financial model requires a knowledge of these diagrams. A single soliton structure includes both dark and bright

solitons. In financing, this structure can be utilized to clarify complex events in the market involving favorable and bearish tendencies, either simultaneously or alternately, and it may help traders in dealing with volatile market conditions by predicting fluctuations in markets which include both upward and downward oscillations.

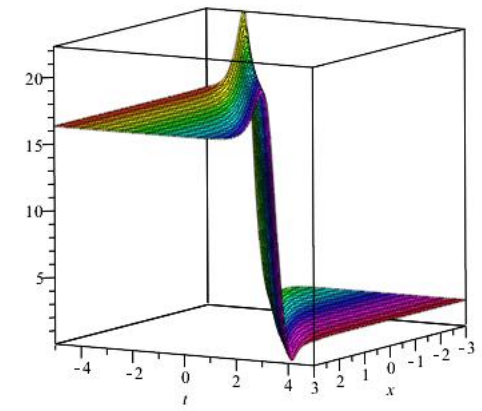

(a) 3D plot of V_3 at $\alpha = 0.9$.

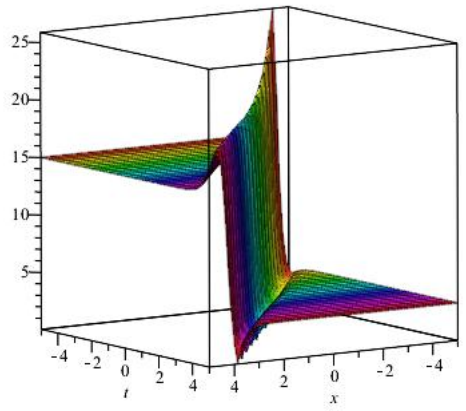

(b) 3D plot of U_3 at $\alpha = 0.9$.

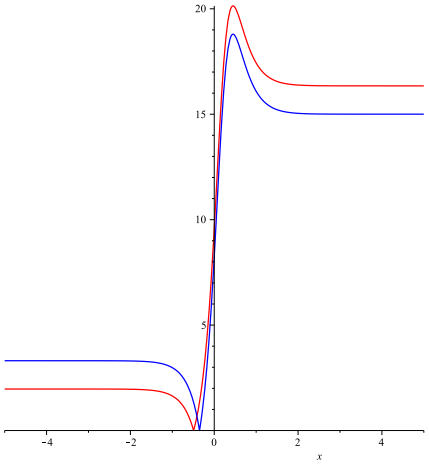

(c) ____ (V_3) ____ (U_3) at $\alpha = 0.9$.

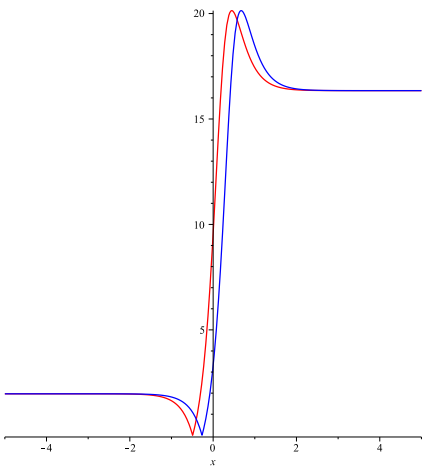

(d) V_3 at ____ $(\alpha = 0.9)$ ____ $(\alpha = 0.7)$.

Figure 2. Graphical representation of combined dark-bright soliton solution for V_3 and U_3 with $\beta = 1$, $\gamma = 0.6$, $c = 1$, $\theta = 0.8$, $\omega_0 = 0.1$, $\omega_1 = 0.1$, and different values of α.

The combined dark-singular soliton solution for V_5 and U_5 is depicted graphically in Figure 3. 3D graphs of V_5 and U_5 at $\alpha = 0.8$, a comparison of their solutions, and a comparison of V_5 at $\alpha = 0.8$ and $\alpha = 0.45$ make up this presentation. The combined dark-singular soliton may be capable to observe complex market dynamics in distinct, focused disruptions. For investors as well as traders, it may be highly enlightening for understanding the actions and relationships of variables such as V_5 and U_5 inside the financial model. Further, it enhances decision-making and assists with modeling, which allows stakeholders in the financial sector in navigating the system with broadened expertise.

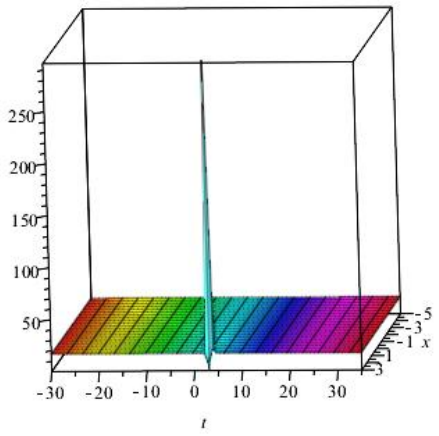

(a) 3D plot of V_5 at $\alpha = 0.8$.

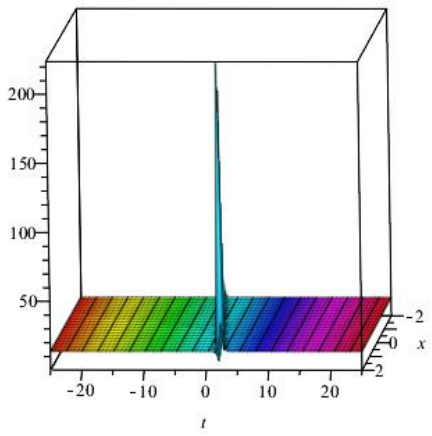

(b) 3D plot of U_5 at $\alpha = 0.8$.

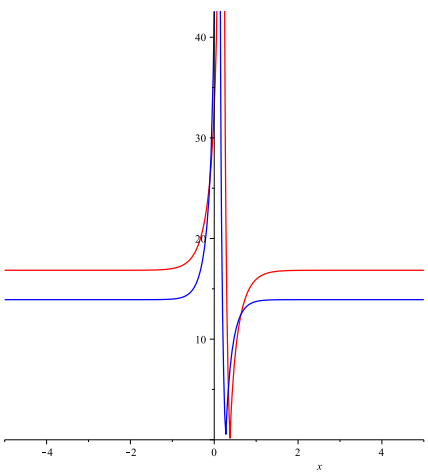

(c) ____ (V_5) ____ $(U_5(x,t))$ at $\alpha = 0.8$.

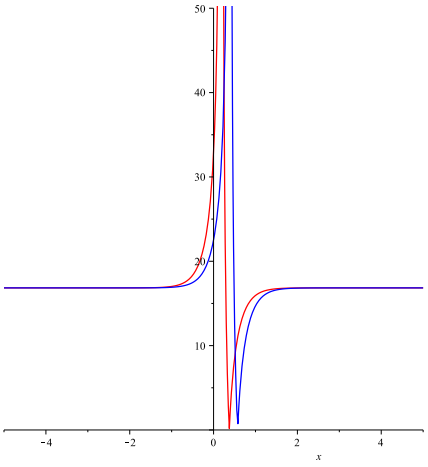

(d) V_5 at ____ $(\alpha = 0.8)$ ____ $(\alpha = 0.45)$.

Figure 3. Graphical representation of combined dark-singular soliton solution for V_5 and U_5 with $\beta = 1$, $\gamma = 0.6$, $c = 1$, $\theta = 0.8$, $\omega_0 = 0.1$, $\omega_1 = 0.1$, and different values of α.

The visual illustration in Figure 4 portrays the periodic-singular soliton for V_{14} and U_{14}. The selection of visualizations encompasses 3D plots demonstrating V_{14} and U_{14} at $\alpha = 0.8$. Likewise, a comparative analysis at $\alpha = 0.8$ indicates the correlation among the solutions of V_{14} and U_{14} in the financial model. Ultimately, it highlights V_{14} at two independent values of α, particularly $\alpha = 0.8$ and $\alpha = 0.5$. Understanding the periodic-singular soliton in financial modeling is essential to express the oscillations related to external shocks or transforms in economic cycles.

The diagram in Figure 5 highlights the singular soliton solution for V_{27} and U_{27}. 3D graphs of V_{27} and U_{27} at $\alpha = 0.7$, a comparison of their solutions, and a comparison of V_{27} at $\alpha = 0.7$ and $\alpha = 0.5$ make up this presentation. Localized disturbance is demonstrated by singular solitons and they have an essential role in financial modeling. These interruptions may be caused by multiple factors such as unexpected fluctuations in stocks and changing behavior of investors.

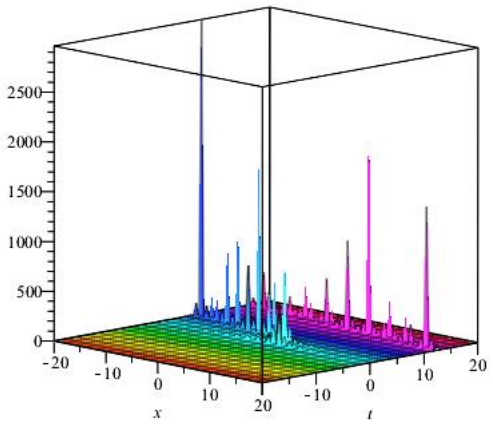

(a) 3D plot of V_{14} at $\alpha = 0.8$.

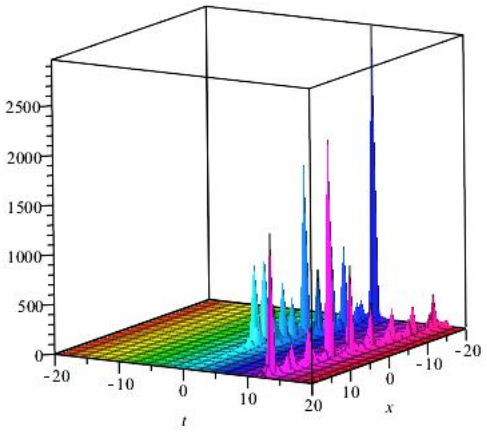

(b) 3D plot of U_{14} at $\alpha = 0.8$.

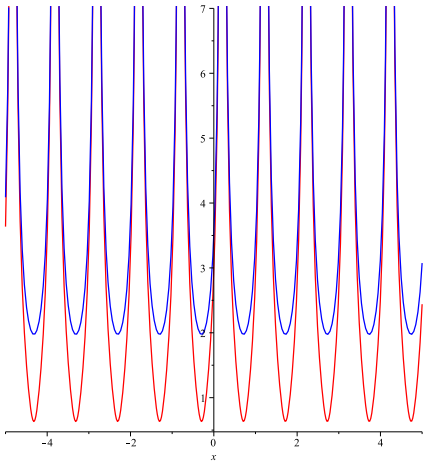

(c) ____ (V_{14}) ____ (U_{14}) at $\alpha = 0.8$.

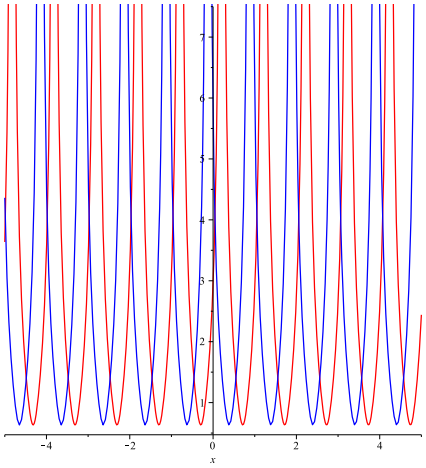

(d) V_{14} at ____ ($\alpha = 0.8$) ____ ($\alpha = 0.5$).

Figure 4. Graphical representation of periodic-singular soliton solution for V_{14} and U_{14} with $\beta = 1$, $\gamma = 0.6$, $c = 1$, $\theta = 0.8$, $\omega_0 = 0.1$, $\omega_1 = 0.1$, and different values of α.

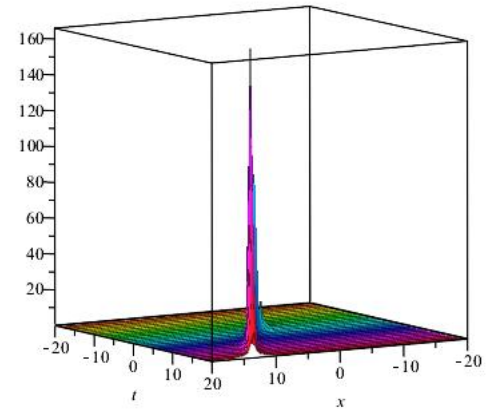

(a) 3D plot of V_{27} at $\alpha = 0.7$.

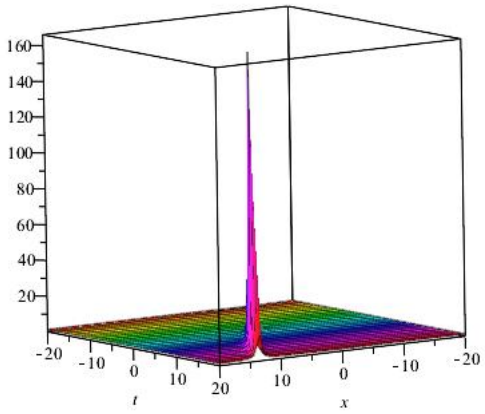

(b) 3D plot of U_{27} at $\alpha = 0.7$.

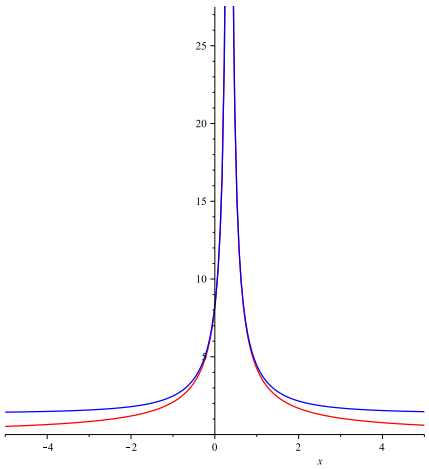

(c) ____ (V_{27}) ____ (U_{27}) at $\alpha = 0.7$.

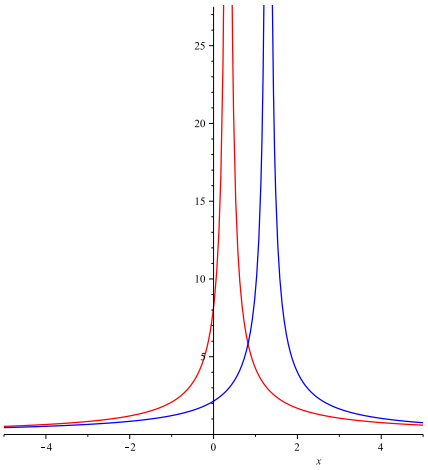

(d) V_{27} at ____ $(\alpha = 0.7)$ ____ $(\alpha = 0.5)$.

Figure 5. Graphical representation of singular soliton solution for V_{27} and U_{27} with $\beta = 1$, $\gamma = 0.6$, $c = 1$, $c_1 = 1$, $\theta = 0.8$, $\omega_0 = 0.1$, $\omega_1 = 0.1$, and different values of α.

The bright soliton solution for $V_{1,2}$ and $U_{1,2}$ is shown graphically in Figure 6. 3D graphs of $V_{1,2}$ and $U_{1,2}$ at $\alpha = 0.8$, a comparison of their solutions, and a comparison of $V_{1,2}$ at $\alpha = 0.8$ and $\alpha = 0.5$ make up this presentation. Bright solitons demonstrate high intensity at their peaks that can be linked to specific asset price trends or incidents, such as unexpected rises or falls in value.

Hence, the integration of fractional calculus into option pricing models offers a more realistic depiction of financial market dynamics, enhancing risk management strategies and enabling more informed decision-making. Soliton solutions improve market forecasting and option valuation, aiding financial institution in minimizing risk and maximizing returns. Beyond finance, our research contributes to fields such as signal processing, telecommunication, material science, biomedical engineering, and environmental sciences. For instance, soliton behavior can enhance signal integrity in telecommunications and model complex materials' properties. In addition, understanding wave

propagation in biological tissues can improve medical imaging and diagnostics. The adoption of these models across industries can lead to significant technological advancements, including enhanced financial software, innovative engineering solutions, and improved diagnostic tools, thereby driving progress and innovation across multiple domains.

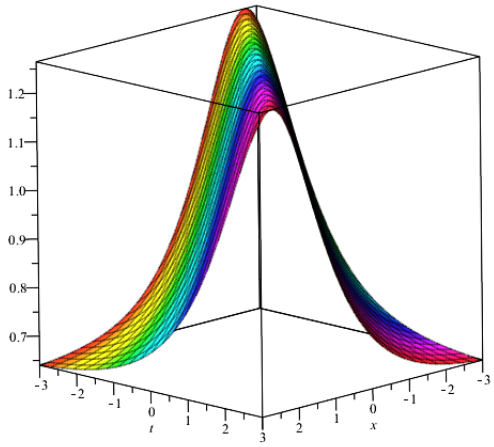

(a) 3D plot of $V_{1,2}$ at $\alpha = 0.8$.

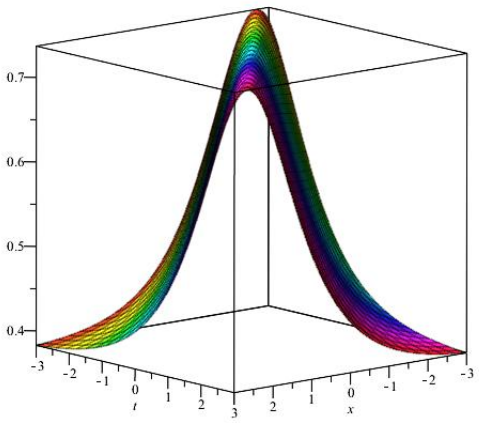

(b) 3D plot of $U_{1,2}$ at $\alpha = 0.8$.

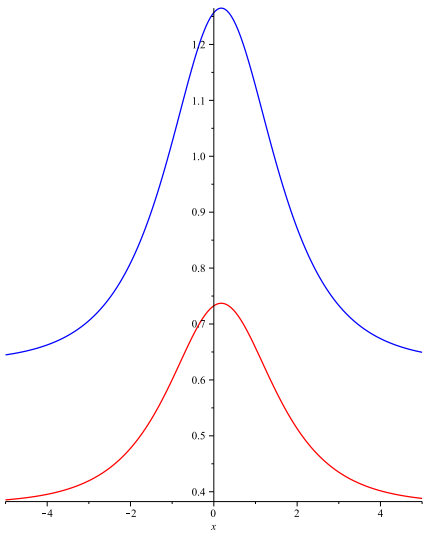

(c) ——— $(V_{1,2})$ ——— $(U_{1,2})$ at $\alpha = 0.8$.

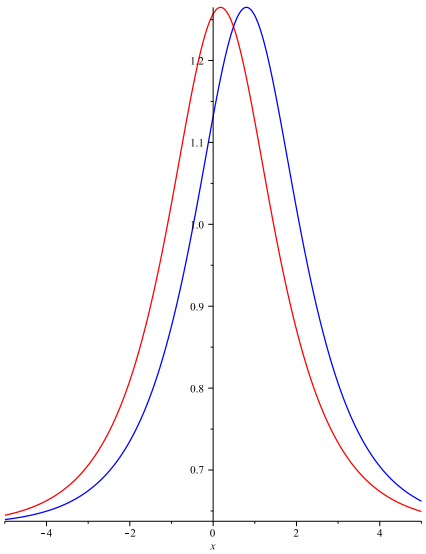

(d) $V_{1,2}$ at ——— $(\alpha = 0.8)$ ——— $(\alpha = 0.5)$.

Figure 6. Graphical representation of bright soliton solution for $V_{1,2}$ and $U_{1,2}$ with $\beta = 1$, $\gamma = 0.6$, $c = 1$, $\theta = 0.8$, and different values of α.

7. Conclusions

The intricate nature and stochastic characteristics in option pricing problems pose challenges in obtaining the precise value of options. Consequently, there is a need for precise approximation

techniques to comprehend the intricacies of these problems. Such methods play a crucial role in advancing scientific understanding within financial markets, contributing significantly to ongoing developments in the field. The model under study emerges as a novel fractional nonlinear coupled wave alternative to the established Black-Scholes option pricing framework. This groundbreaking innovation introduces a leveraging effect, aligning stock volatility with stock returns through the utilization of GREM and NKM. The study reveals the successful generation of kink, dark, bright, periodic-singular, singular, dark-singular, and dark-bright solitons. Notably, altering the fractional order induces left or right shifts in the graphs, along with changes in amplitude. The comparison between two profiles reveals distinctive phase components and amplitude differences. This comprehensive investigation positions the proposed method as a reliable and versatile solution, preserving the inherent physical attributes of realistic processes within the domain of option pricing. In summary, the main findings of our study highlight a fractional nonlinear coupled wave system as an alternative to the Black-Scholes option pricing model, which enhances the accuracy and flexibility in modeling market dynamics. The generalized Ricatti mapping and new Kudryashov methods effectively generate novel solitonic wave structures, and the graphical representations aid in understanding pulse propagation and parameter alignment with observed data. Comparative analysis of different fractional order values validates the flexibility of our proposed methods.

Author contributions

H. U. Rehman, P. J. Y. Wong and M. S. Saleem: Formal analysis, Investigation, Writing-original draft; H. U. Rehman, P. J. Y. Wong and I. Iqbal: Revision; H. U. Rehman, P. J. Y. Wong, A. F. Aljohani, I. Iqbal and M. S. Saleem: Writing-review & editing. All authors have read and agreed to the published version of the manuscript.

Use of AI tools declaration

The authors declare they have not used Artificial Intelligence (AI) tools in the creation of this article.

Conflict of interest

Dr. Patricia J. Y. Wong is the Guest Editor of special issue "Partial Differential Equations–Theory, methods and applications" for AIMS Mathematics. Patricia J. Y. Wong was not involved in the editorial review and the decision to publish this article.

The authors declare no conflicts of interest.

References

1. J. C. Zhao, M. Davison, R. M. Corless, Compact finite difference method for American option pricing, *J. Comput. Appl. Math.*, **206** (2007), 306–321. https://doi.org/10.1016/j.cam.2006.07.006
2. D. C. Lesmana, S. Wang, An upwind finite difference method for a nonlinear Black-Scholes equation governing European option valuation under transaction costs, *Appl. Math. Comput.*, **219** (2013), 8811–8828. https://doi.org/10.1016/j.amc.2012.12.077

3. J. A. Rad, K. Parand, S. Abbasbandy, Local weak form meshless techniques based on the radial point interpolation (RPI) method and local boundary integral equation (LBIE) method to evaluate European and American options, *Commun. Nonlinear Sci. Numer. Simul.*, **22** (2015), 1178–1200. https://doi.org/10.1016/j.cnsns.2014.07.015
4. F. Black, M. Scholes, The pricing of options and corporate liabilities, *J. Polit. Econ.*, **81** (1973), 637–654. https://doi.org/10.1142/9789814759588_0001
5. R. C. Merton, Theory of rational option pricing, *Bell J. Econ. Manag. Sci.*, **4** (1973), 141–183. https://doi.org/10.1142/9789814759588_0002
6. H. Mesgarani, M. Bakhshandeh, Y. E. Aghdam, J. F. Gómez-Aguilar, The convergence analysis of the numerical calculation to price the time-fractional Black-Scholes model, *Comput. Econ.*, **62** (2023), 1845–1856. https://doi.org/10.1007/s10614-022-10322-x
7. P. P. Boyle, T. Vorst, Option replication in discrete time with transaction costs, *J. Finance*, **47** (1992), 271–293. https://doi.org/10.1111/j.1540-6261.1992.tb03986.x
8. H. E. Leland, Option pricing and replication with transactions costs, *J. Finance*, **40** (1985), 1283–1301. https://doi.org/10.1111/j.1540-6261.1985.tb02383.x
9. G. Barles, H. M. Soner, Option pricing with transaction costs and a nonlinear Black-Scholes equation, *Finance Stoch.*, **2** (1998), 369–397. https://doi.org/10.1007/s007800050046
10. S. Kusuoka, Limit theorem on option replication cost with transaction costs, *Ann. Appl. Probab.*, **5** (1995), 198–221. https://doi.org/10.1214/aoap/1177004836
11. V. G. Ivancevic, Adaptive-wave alternative for the Black-Scholes option pricing model, *Cogn. Comput.*, **2** (2010), 17–30. https://doi.org/10.1007/s12559-009-9031-x
12. A. S. Suresh, S. N. Prasath, A study to understand Elliott wave principle, *Int. J. Eng. Res. Gen. Sci.*, **4** (2016), 352–363.
13. A. W. Lo, Reconciling efficient markets with behavioral finance: the adaptive markets hypothesis, *J. Invest. Consult.*, **7** (2005), 21–44.
14. S. C. Kak, Quantum neural computing, *Adv. Imaging Electron Phys.*, **94** (1995), 259–313. https://doi.org/10.1016/S1076-5670(08)70147-2
15. O. González-Gaxiola, S. O. Edeki, O. O. Ugbebor, J. R. de Chávez, Solving the Ivancevic pricing model using the He's frequency amplitude formulation, *Eur. J. Pure Appl. Math.*, **10** (2017), 631–637.
16. Q. L. Chen, H. M. Baskonus, W. Gao, E. Ilhan, Soliton theory and modulation instability analysis: the Ivancevic option pricing model in economy, *Alexandria Eng. J.*, **61** (2022), 7843–7851. https://doi.org/10.1016/j.aej.2022.01.029
17. K. K. Ali, M. A. Maaty, M. Maneea, Optimizing option pricing: exact and approximate solutions for the time-fractional Ivancevic model, *Alexandria Eng. J.*, **84** (2023), 59–70. https://doi.org/10.1016/j.aej.2023.10.066
18. Z. Y. Yan, Financial rogue waves appearing in the coupled nonlinear volatility and option pricing model, 2011, arXiv: 1101.3107.

19. M. B. Riaz, A. R. Ansari, A. Jhangeer, M. Imran, C. K. Chan, The fractional soliton wave propagation of non-linear volatility and option pricing systems with a sensitive demonstration, *Fractals Fract.*, **7** (2023), 1–28. https://doi.org/10.3390/fractalfract7110809

20. B. Acay, E. Bas, T. Abdeljawad, Non-local fractional calculus from different viewpoint generated by truncated *M*-derivative, *J. Comput. Appl. Math.*, **366** (2020), 112410. https://doi.org/10.1016/j.cam.2019.112410

21. K. Diethelm, N. J. Ford, Analysis of fractional differential equations, *J. Math. Anal. Appl.*, **265** (2002), 229–248. https://doi.org/10.1006/jmaa.2000.7194

22. P. C. Ma, A. Najafi, J. F. Gomez-Aguilar, Sub mixed fractional Brownian motion and its application to finance, *Chaos Solitons Fract.*, **184** (2024), 114968. https://doi.org/10.1016/j.chaos.2024.114968

23. A. A. Kilbas, H. M. Srivastava, J. J. Trujillo, *Theory and applications of fractional differential equations*, Amsterdam: Elsevier, 2006.

24. A. Goswami, J. Singh, D. Kumar, Sushila, An efficient analytical approach for fractional equal width equations describing hydro-magnetic waves in cold plasma, *Phys. A*, **524** (2019), 563–575. https://doi.org/10.1016/j.physa.2019.04.058

25. A. Goswami, Sushila, J. Singh, D. Kumar, Numerical computation of fractional Kersten-Krasil'shchik coupled KdV-mKdV system occurring in multi-component plasmas, *AIMS Math.*, **5** (2020), 2346–2368. https://doi.org/10.3934/math.2020155

26. H. U. Rehman, M. I. Asjad, I. Iqbal, A. Akgül, Soliton solutions of space-time fractional Zoomeron differential equation, *Int. J. Appl. Nonlinear Sci.*, **4** (2023), 29–46. https://doi.org/10.1504/IJANS.2023.133734

27. M. I. Asjad, N. Ullah, H. U. Rehman, T. N. Gia, Novel soliton solutions to the Atangana-Baleanu fractional system of equations for the ISALWs, *Open Phys.*, **19** (2021), 770–779. https://doi.org/10.1515/phys-2021-0085

28. D. Shi, H. U. Rehman, I. Iqbal, M. Vivas-Cortez, M. S. Saleem, X. J. Zhang, Analytical study of the dynamics in the double-chain model of DNA, *Results Phys.*, **52** (2023), 106787. https://doi.org/10.1016/j.rinp.2023.106787

29. H. U. Rehman, A. U. Awan, E. M. Tag-ElDin, S. E. Alhazmi, M. F. Yassen, R. Haider, Extended hyperbolic function method for the (2+1)-dimensional nonlinear soliton equation, *Results Phys.*, **40** (2022), 105802. https://doi.org/10.1016/j.rinp.2022.105802

30. H. Zhao, J. G. Han, W. T. Wang, H. Y. An, Applications of extended hyperbolic function method for quintic discrete nonlinear Schrödinger equation, *Commun. Theor. Phys.*, **47** (2007), 474. https://doi.org/10.1088/0253-6102/47/3/020

31. H. U. Rehman, I. Iqbal, S. Subhi Aiadi, N. Mlaiki, M. S. Saleem, Soliton solutions of Klein-Fock-Gordon equation using Sardar subequation method, *Mathematics*, **10** (2022), 1–10. https://doi.org/10.3390/math10183377

32. I. Iqbal, H. U. Rehman, M. Mirzazadeh, M. S. Hashemi, Retrieval of optical solitons for nonlinear models with Kudryashov's quintuple power law and dual-form nonlocal nonlinearity, *Opt. Quantum Electron.*, **55** (2023), 588. https://doi.org/10.1007/s11082-023-04866-x

33. H. U. Rehman, N. Ullah, M. A. Imran, Highly dispersive optical solitons using Kudryashov's method, *Optik*, **199** (2019), 163349.

34. P. N. Ryabov, D. I. Sinelshchikov, M. B. Kochanov, Application of the Kudryashov method for finding exact solutions of the high order nonlinear evolution equations, *Appl. Math. Comput.*, **218** (2011), 3965–3972. https://doi.org/10.1016/j.amc.2011.09.027

35. M. A. Salam, M. S. Uddin, P. Dey, Generalized Bernoulli sub-ODE method and its applications, *Ann. Pure Appl. Math.*, **10** (2015), 1–6.

36. B. Zheng, A new Bernoulli sub-ODE method for constructing traveling wave solutions for two nonlinear equations with any order, *U.P.B. Sci. Bull. Ser. A*, **73** (2011), 85–94.

37. S. K. Liu, Z. T. Fu, S. D. Liu, Q. Zhao, Jacobi elliptic function expansion method and periodic wave solutions of nonlinear wave equations, *Phys. Lett. A*, **289** (2001), 69–74. https://doi.org/10.1016/S0375-9601(01)00580-1

38. S. A. Allahyani, H. U. Rehman, A. U. Awan, E. M. Tag-ElDin, M. U. Hassan, Diverse variety of exact solutions for nonlinear Gilson-Pickering equation, *Symmetry*, **14** (2022), 1–15. https://doi.org/10.3390/sym14102151

39. H. U. Rehman, N. Ullah, M. A. Imran, Optical solitons of Biswas-Arshed equation in birefringent fibers using extended direct algebraic method, *Optik*, **226** (2021), 165378. https://doi.org/10.1016/j.ijleo.2020.165378

40. A. Kurt, A. Tozar, O. Tasbozan, Applying the new extended direct algebraic method to solve the equation of obliquely interacting waves in shallow waters, *J. Ocean Univ. China*, **19** (2020), 772–780. https://doi.org/10.1007/s11802-020-4135-8

41. H. U. Rehman, M. S. Saleem, M. Zubair, S. Jafar, I. Latif, Optical solitons with Biswas-Arshed model using mapping method, *Optik*, **194** (2019), 163091. https://doi.org/10.1016/j.ijleo.2019.163091

42. X. Zeng, X. L. Yong, A new mapping method and its applications to nonlinear partial differential equations, *Phys. Lett. A*, **372** (2008), 6602–6607. https://doi.org/10.1016/j.physleta.2008.09.025

43. W. W. Mohammed, C. Cesarano, The soliton solutions for the (4+1)-dimensional stochastic Fokas equation, *Math. Methods Appl. Sci.*, **46** (2023), 7589–7597. https://doi.org/10.1002/mma.8986

44. W. W. Mohammed, F. M. Al-Askar, C. Cesarano, The analytical solutions of the stochastic mKdV equation via the mapping method, *Mathematics*, **10** (2022), 1–9. https://doi.org/10.3390/math10224212

45. M. U. Shahzad, H. U. Rehman, A. U. Awan, Z. Zafar, A. M. Hassan, I. Iqbal, Analysis of the exact solutions of nonlinear coupled Drinfeld-Sokolov-Wilson equation through ϕ^6-model expansion method, *Results Phys.*, **52** (2023), 106771. https://doi.org/10.1016/j.rinp.2023.106771

46. N. Ahmed, M. Z. Baber, M. S. Iqbal, A. Annum, S. M. Ali, M. Ali, et al., Analytical study of reaction diffusion Lengyel-Epstein system by generalized Riccati equation mapping method, *Sci. Rep.*, **13** (2023), 20033. https://doi.org/10.1038/s41598-023-47207-4

47. H. Naher, F. A. Abdullah, S. T. Mohyud-Din, Extended generalized Riccati equation mapping method for the fifth-order Sawada-Kotera equation, *AIP Adv.*, **3** (2013), 052104. https://doi.org/10.1063/1.4804433

48. H. U. Rehman, G. S. Said, A. Amer, H. Ashraf, M. M. Tharwat, M. Abdel-Aty, et al., Unraveling the (4+1)-dimensional Davey-Stewartson-Kadomtsev-Petviashvili equation: exploring soliton solutions via multiple techniques, *Alex. Eng. J.*, **90** (2024), 17–23. https://doi.org/10.1016/j.aej.2024.01.058

49. H. J. Haubold, A. M. Mathai, R. K. Saxena, Mittag-Leffler functions and their applications, *J. Appl. Math.*, **2011** (2011), 298628. https://doi.org/10.1155/2011/298628

50. J. Zhang, X. L. Wei, Y. J. Lu, A generalized (G'/G)-expansion method and its applications, *Phys. Lett. A*, **372** (2008), 3653–3658. https://doi.org/10.1016/j.physleta.2008.02.027